J. Comput. Appl. Res. Mech. Eng. Vol. 13. No. 1, pp. 89-101, 2023 *DOI: 10.22061/JCARME.2023.8944.2207*

SRTTU

Journal of Computational and Applied Research in Mechanical Engineering

jcarme.sru.ac.ir

JCARME

ISSN: 2228-7922

Research paper

Numerical investigation of the effect of size distribution on the frequency response of encapsulated microbubbles

M. Mahdi[a*], M. Shariatnia and M. Rahimi

[a]*Department of Mechanical Engineering, Shahid Rajaee Teacher Training University, Tehran, Iran*

Article info:

Article history:

Received: 14/04/2022

Accepted: 09/05/2023

Revised: 12/05/2023

Online: 14/05/2023

Keywords:

Ultrasound contrast agent,

Frequency response,

Subharmonic response,

Size distribution,

Gaussian distribution.

[*]Corresponding author:

m.mahdi@sru.ac.ir

Abstract

Microbubbles are used in ultrasound imaging, targeted drug delivery, destruction of cancerous tissues, etc. On the other hand, the demographic behaviors of small bubbles under the influence of Ultrasound have not been fully detected or studied. This study investigates the effect of the radial distribution of Sonazoid microbubbles on frequency response. It is shown that the optimal subharmonic response is possible by controlling the size distribution. For this reason, the numerical simulation of the dynamic behavior of a coated microbubble is performed using MATLAB coding and the modified Rayleigh-Plesset equation. The Gaussian distribution is then applied, and the frequency response is investigated. It was shown that at a constant excitation pressure of 0.4 MPa and a standard deviation of 0.2, with increasing mean radius, the fundamental response increases. The subharmonic response increases reaches a peak value and decreases. This peak value occurs for frequencies of 4,6, and 8 MHz in the mean radius of 0.8, 1 and 1.6 μm. By increasing the frequency of excitation, it is transferred to a smaller mean radius. It is also observed that the fundamental and subharmonic responses are amplified by increasing the excitation pressure. Studies show that the optimal subharmonic response can be achieved for various applications by controlling the size distribution of microbubbles.

1. Introduction

During the past years, encapsulated microbubbles have been used in Ultrasound imaging and therapy. Due to the difference in acoustic impedance, these microbubbles cause the scattering and reflection of ultrasound waves sent from the targeted place. Blood is a poor reflector of ultrasound, therefore, to improve these properties, microbubbles in micron size are injected intravenously into the blood flow.

Microbubble contrast agents (1 to 10 μm) are stabilized with a shell (lipid or albumin). Rayleigh-Plesset (RP) equation is used to simulate the radial behavior of a free bubble. However, this equation changes for the encapsulated microbubble that includes the shell.

De Jong *et al.* [1] did a different study on the RP equation and investigated the effect of the shell on the radial behavior of the bubble and proposed two parameters, the shell elasticity

parameter (S_p) and the shell friction (S_f) to correct it. By presenting a theoretical model for the radial behavior of an encapsulated microbubble in a Newtonian fluid, Church [2] found that the resonance frequency of the microbubble increases with the addition of a shell and increases the rigidity of the microbubble [3, 4]. Hoff *et al.* [5] obtained a new model for the size changes of an encapsulated microbubble with a thin shell thickness, which predicted the acoustic scattering caused by the radial oscillation of the bubble. Chatterjee *et al.* [6] proposed the simplest Newtonian model for the enclosed microbubble shell. Shankar *et al.* [7] showed that the threshold pressure value for subharmonic onset depends on the actual damping value. Finally, Sarkar *et al.* [8] investigated the scattering responses by presenting a viscoelastic interface model for a microbubble enclosed by a thin shell.

Marmottant *et al.* [9] proposed a model that simulates the nonlinear behavior of an encapsulated microbubble at high excitation pressure by considering three different states for bubble surface tension. The investigation of Forsberg *et al.* [10, 11] showed that the subharmonic response significantly depends on the excitation and hydrostatic pressure amplitude. The advantages of subharmonic response, which is a microbubble contrast agent, were investigated by Shankar *et al.* [12]. Adam *et al.* [13] numerically investigated the effect of ambient pressure on the acoustic scattering of Optison. The subharmonic response of a microbubble contrast agent as a function of ambient pressure was investigated experimentally by Andersen and Jensen [14]. By investigating the effects of pressure and frequency, Katiyar *et al.* [15] achieved a critical frequency ratio with peak subharmonic response. The studies of Leodore *et al.* [16] showed that there is a correlation between the amplitude of the subharmonic component and the hydrostatic pressure in the growth phase of the subharmonic generation.

Microbubbles are available in imaging applications in different radial sizes, and the size of the microbubble radius is an essential factor in the microbubble frequency response. Overvelde *et al.* [17] experimented with the subharmonic behavior of phospholipid microbubbles of various sizes. They also studied the subharmonic threshold using the Marmottant model, and the results showed that at low pressures and a moving frequency twice the frequency of the bubble intensification, the subharmonic response occurred. Moreover, they showed that the change in bubble shell elasticity as a function of bubble radius increases the subharmonic behavior of microbubbles. Sun *et al.* [18] addressed the dependence of the ultra-harmonic response and the overpressure using experimental and theoretical measurements. They also examined the relationship between subharmonic and ultra-harmonic responses to excitation frequency and pressure amplitude. They concluded that for microbubbles with size distribution, the subharmonic and ultra-harmonic responses could be reduced or increased by increasing the ambient pressure and excitation frequency. The strength of these responses was proportional to the excitation pressure amplitude. Basude and Wheatly [19] obtained the radial distribution of the ultrasound contrast agents with the ST68-PFC Surfactant shell, studied the frequency response, and found that the subharmonic and ultra-harmonic responses Increased with increasing excitation pressure. Frinking *et al.* [20] examined the subharmonic response of phospholipid microbubbles (such as SonoVue) using the Marmottant model. They found that subharmonic components and "compression-only" behavior are observed by applying ambient pressure. Moreover, the increase of the sub-harmonic amplitude is a function of the ambient pressure.

Lotsberg *et al.* [21] investigated the nonlinear emission of the encapsulated bubble experimentally and presented the obtained results with an emphasis on the subharmonic emission. They stimulated clouds of bubbles with a frequency of 3.5 to 4 MHz and observed that the subharmonic component increases with excitation pressure cube in the range of 50 to 100 kPa. Zheng and Shandas [22] defined a modified model of the Rayleigh-Plesset Equation. Moreover, they investigated the frequency response of the radial distribution of Levovist and ST68 microbubbles experimentally and

theoretically. Moreover, they optimized the excitation pressure with a radius for subharmonic, ultra-harmonic, and second-harmonic responses. Numerical investigation of the characteristics of nonlinear acoustic emission from a coated bubble was done by Zhang *et al.* [23]. They showed that bubble size has a significant effect on the type of bubble acoustic emission. Newsome *et al.* [24] mathematically investigated the effect of the size distribution of bubbles on the propagation of acoustic waves. Haghi *et al.* [25] found that by increasing the diameter of the microbubbles from 1 to 4 micrometers, the superharmonic response decreases. Streeter *et al.* [26] Investigated the nonlinear behavior of a polydisperse microbubble cluster. They showed that the largest microbubbles could force smaller ones into period-doubling and subharmonic oscillations. Tsochatzidis *et al.* [27] performed perfusion and molecular imaging studies with microbubbles in sorted diameters of 1.1 ± 0.43 μm and 3.3 ± 1.95 μm and unsorted state (0.9 ± 0.45 μm) to investigate the effect of diameter of microbubbles of contrast agents on imaging sensitivity. They showed that tailoring size distributions improve imaging sensitivity over unsorted populations.

Determining the size distribution of microbubbles in the liquid is essential for studying the multi-dispersion bubble system. The simplest method is to experimentally measure the bubble size distribution in the liquid and use a histogram. This method works very well in laboratory studies but is not applicable in engineering applications due to the associated costs. Also, measuring an accurate histogram becomes a complex task in some working conditions [28, 29]. By using mathematical functions such as Ando *et al.* [30] and Hilgenfeldt *et al.* [31] bubble size distributions, can be study a multi-scatter bubble system. Other mathematical functions such as Gaussian distribution have a much wider application than previous cases because there are two adjustable parameters in the Gaussian distribution. Gaussian distribution and its parameters are used in this study to investigate the distribution.

Microbubbles are in different radii in applications (especially ultrasound imaging). So far, less attention has been paid to the radial distribution of microbubbles and their effects on the frequency response. In contrast, this subject is used in applications, especially ultrasound imaging. On the other hand, the demographic behaviors of small bubbles under the influence of Ultrasound have not been fully detected or studied. We show in this study that the optimal subharmonic response is possible by controlling the radial distribution. In this research, the modified RP equation is solved with the help of an ODE solver in MATLAB software. We discuss the effects of the radial distribution of microbubbles at different excitation pressures and frequencies on the frequency response. Finally, we show that the radial distribution of microbubbles can lead to different changes in the frequency response and the existence of a maximum value in the subharmonic response. Therefore, controlling the radial distribution of microbubbles can help improve imaging quality.

2. Equations and validation

If the microbubble in the liquid is excited by the ultrasound field and the excitation pressure is large enough, the bubble starts to oscillate. The microbubble oscillations cause radial changes, which the mathematical Equation can simulate. In this research, it is assumed that the bubble is always spherical during pressure fluctuations. The equation governing the behavior of the encapsulated microbubble is based on the RP equation. In these models, viscoelastic terms can be shown as $\gamma(R)$ and $\kappa^s(R)$, the efficient surface tension and efficient dilatational viscosity, respectively. Added terms represent the contributions caused by viscoelastic stresses produced in the encapsulation.

$$\rho\left(R\ddot{R}+\frac{3}{2}\dot{R}^2\right)=P_{G0}\left(\frac{R_0}{R}\right)^{3k}\left(1-\frac{3k\dot{R}}{c}\right)-\frac{2\gamma(R)}{R}-\frac{4\dot{R}}{R^2}\kappa^s(R\ \dot{R})-4\mu\frac{\dot{R}}{R}-P_0+p_A(t) \quad (1)$$

P_0 is the hydrostatic pressure, c is sound speed, and $p_A(t)$ is the sinusoidal excitation pressure. Also, the initial conditions are $(t=0)=R_0$ and $\dot{R}(t=0)=0$.

2.1. Marmottant model

Marmottant *et al.* [9] provided a model for bubble radius oscillation in which surface tension has three different states: the buckling state ($R \le R_{buckling}$), the elastic state ($\gamma(R) = \chi(\frac{A}{A_{buckling}} - 1)$) and the rupture state.

$$\gamma(R) = \begin{cases} 0 & R \le R_{buckling} \\ \chi\left(\frac{R^2}{R_{buckling}^2} - 1\right) & R_{buckling} \le R \le R_{rupture} \\ \sigma_w & R \ge R_{rupture} \end{cases}$$

$$and\ \kappa^s(R) = \kappa^s(constant) \tag{2}$$

It is supposed that $R_{buckling} = R_0$, and on the bubble surface, the pressure is in equilibrium. The modified RP equation for this model is defined as below.

$$\rho\left(R\ddot{R} + \frac{3}{2}\dot{R}^2\right) = \left[P_0 + \frac{2\gamma(R_0)}{R_0}\right]\left(\frac{R_0}{R}\right)^{3\gamma}\left(1 - \frac{3\gamma\dot{R}}{c}\right) - \frac{2\gamma(R)}{R} - \frac{4\dot{R}}{R^2}\kappa^s - 4\mu\frac{\dot{R}}{R} - P_0 + P_A(t) \tag{3}$$

2.2. Radius distribution

The scattered pressure of a spherical microbubble at a distance r from the center can be expressed as follows [32, 33].

$$P_{sc}(r,t) = \rho\frac{R(t)}{r}\left(2\dot{R}(t)^2 + \ddot{R}(t)R(t)\right) \tag{4}$$

We have employed a size-integration (SI) method based on the RP equation to predict the nonlinear emission from a group of microbubbles with a wide size range based on several previous studies [22, 34-36]. The method uses a weighting scheme based on the histogram of bubble size distribution to determine the cumulative backscatter.

$$S(f) = \sum_{k=i}^{j} P_{sc}(r_k.f)w_k\% \tag{5}$$

Here, $w_k\%$ is the number percentage weight of bubbles with size k, $P_{sc}(r_k.f)$ is the scattered pressure from bubbles with size k at a frequency band f, $S(f)$ is the total scattered pressure from bubbles with size ranging from i to j at the frequency band f.
Size distribution is a critical factor in controlling the acoustic response from a bubble population. A Gaussian distribution is a reasonable estimate for the size distribution of many contrast bubbles [37, 38]. The Gaussian distribution equation is given by:

$$PDF = \frac{1}{\sigma\sqrt{2\pi}}\left(e^{\frac{-(R-\mu)^2}{2\sigma^2}}\right) \tag{6}$$

In this Equation, σ expresses standard deviation, and μ is the mean radius.

2.3. Validation of the numerical model

Figs. 1 and 2 are presented by applying a Marmottant nonlinear shell model to the coated bubble dynamic Eq. 3 and then employing Eq. 4. According to C. C.hurch [33], the shell parameters were applied (Shell elastic, $\chi = 0.0263$ N/m and dilatational shell viscosity, $\kappa^s = 9.96 \times 10^{-10}$ Kg/s). Sarkar *et al.* [39] obtained the frequency responses of the fundamental and subharmonic components using Fast Fourier Transform (FFT) and compared them with the experimental results. Fig. 3 shows the solution algorithm schematically.

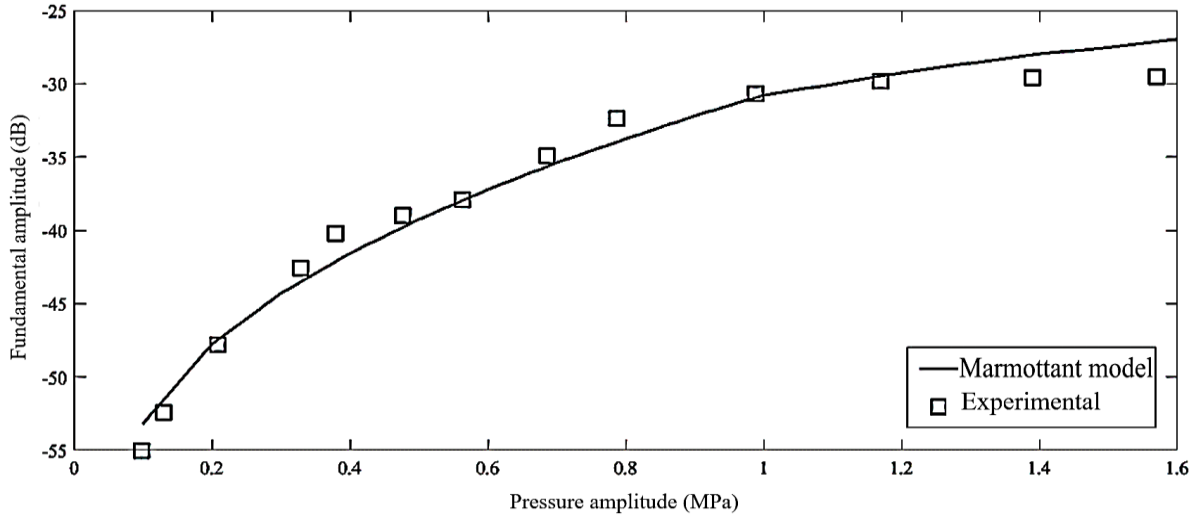

Fig. 1. Fundamental response of the Sonazoid microbubble with the 3 MHz excitation frequency for different excitation pressure amplitudes.

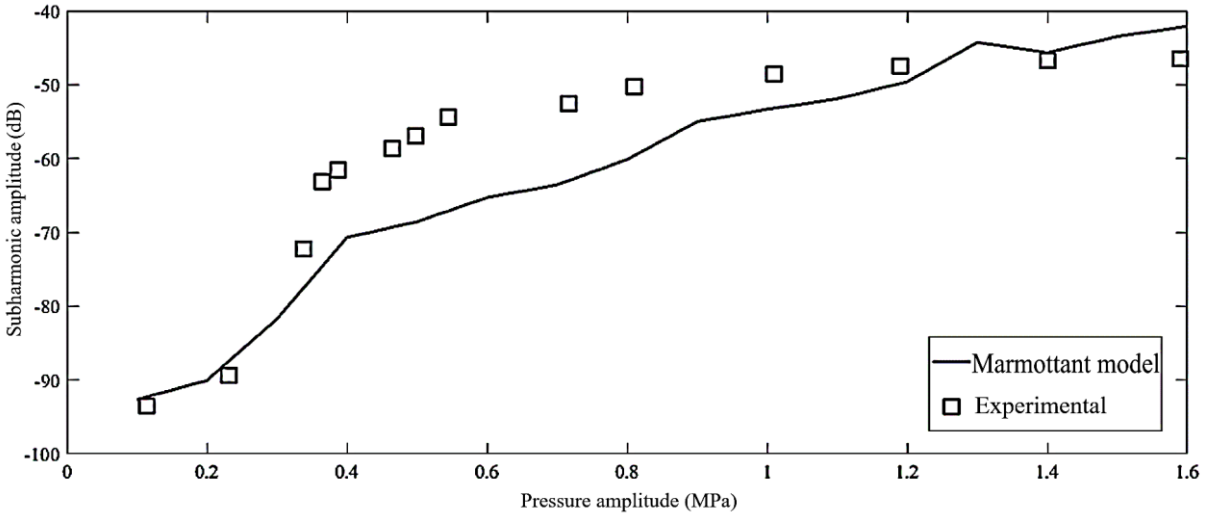

Fig. 2. Subharmonic response of the Sonazoid microbubble with the 3 MHz excitation frequency for different excitation pressure amplitudes.

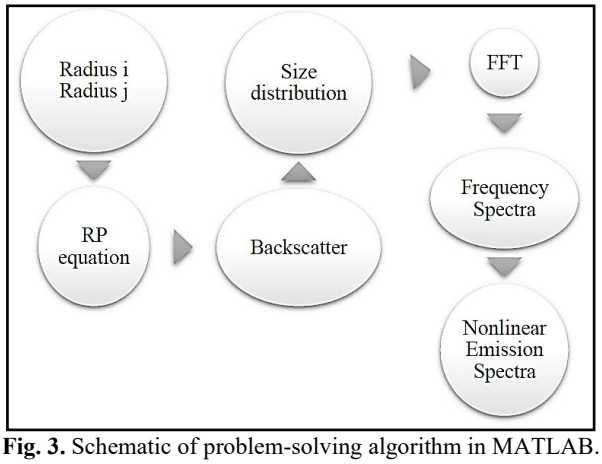

Fig. 3. Schematic of problem-solving algorithm in MATLAB.

3. Results and discussion

Size distribution is paramount for controlling the frequency response of microbubble contrast agents. According to Eq. 6, two dominant parameters control radial size distribution, mean radius and standard deviation. Three different distributions and the frequency response of microbubbles are shown in Figs. 4, 5, and 6. The comparison of Fig. 4 and Fig. 5 shows that the lower standard deviation mode for radial size distribution has more robust subharmonic and ultra-harmonic responses than the higher standard deviation mode (in the range of 5dB for Fig. 4 vs. 5). The subharmonic and ultra-harmonic responses are weakened by increasing the radial amplitude. Figs. 5 and 6 show the population of microbubbles with the same standard deviation and different mean radii. Larger microbubbles emit higher harmonic responses than smaller microbubbles, so the fundamental response is amplified in the size distribution with a larger mean radius.

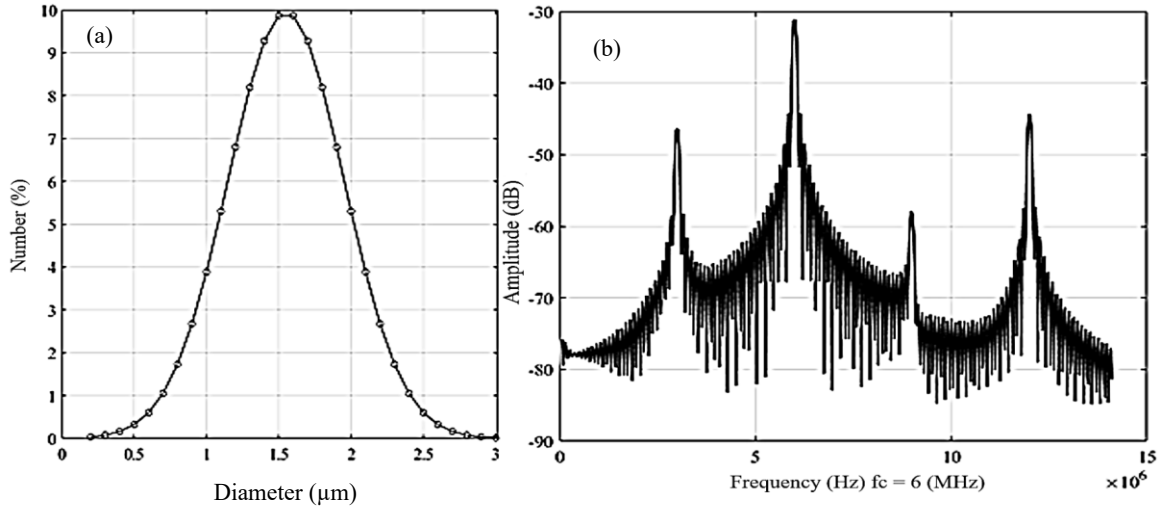

Fig. 4. (a) Gaussian distribution of microbubbles with the mean radius of 0.8 μm and standard deviation of 0.2 μm and (b) Frequency response of microbubbles with this distribution under a driving pressure of 0.28 MPa.

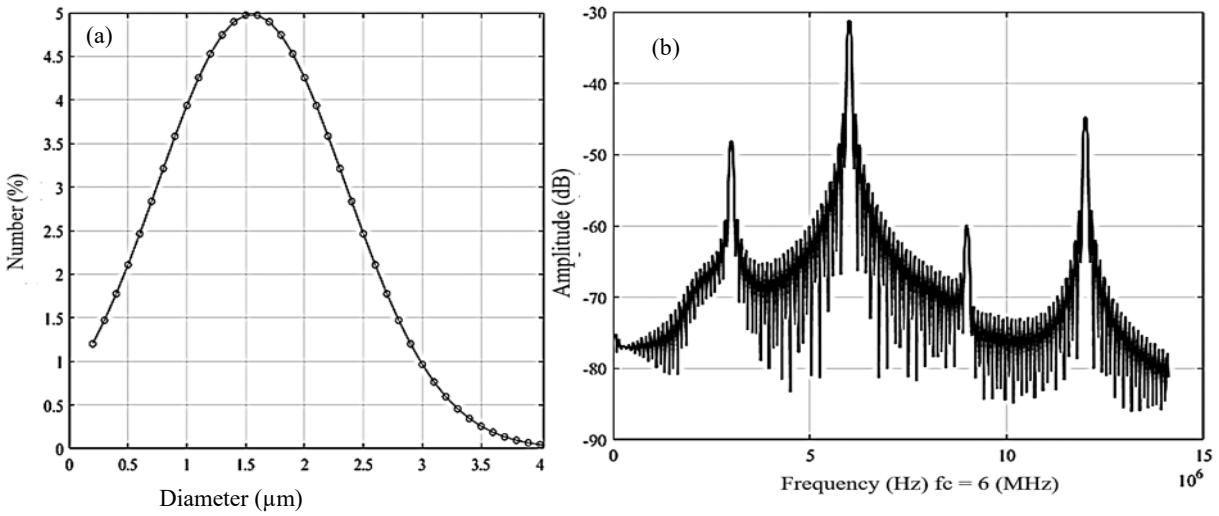

Fig. 5. (a) Gaussian distribution of microbubbles with the mean radius of 0.8 μm and standard deviation of 0.4 μm and (b) Frequency response of microbubbles with this distribution under a driving pressure of 0.28 MPa.

The effect of excitation pressure on the frequency response is essential. Figs. 7 and 8 show the subharmonic and fundamental amplitudes for the mean radii at excitation pressures of 280, 340, and 400kPa. It is observed that the fundamental and subharmonic responses increase with increasing stimulation pressure. Fig. 8 shows that the subharmonic response occurs at a mean radius of 1 μm maximum. This peak value remains constant with increasing excitation pressure at a mean radius of 1 (μm). When the predominant size of the microbubbles becomes smaller or larger than this radius, the subharmonic signal strength decreases significantly.

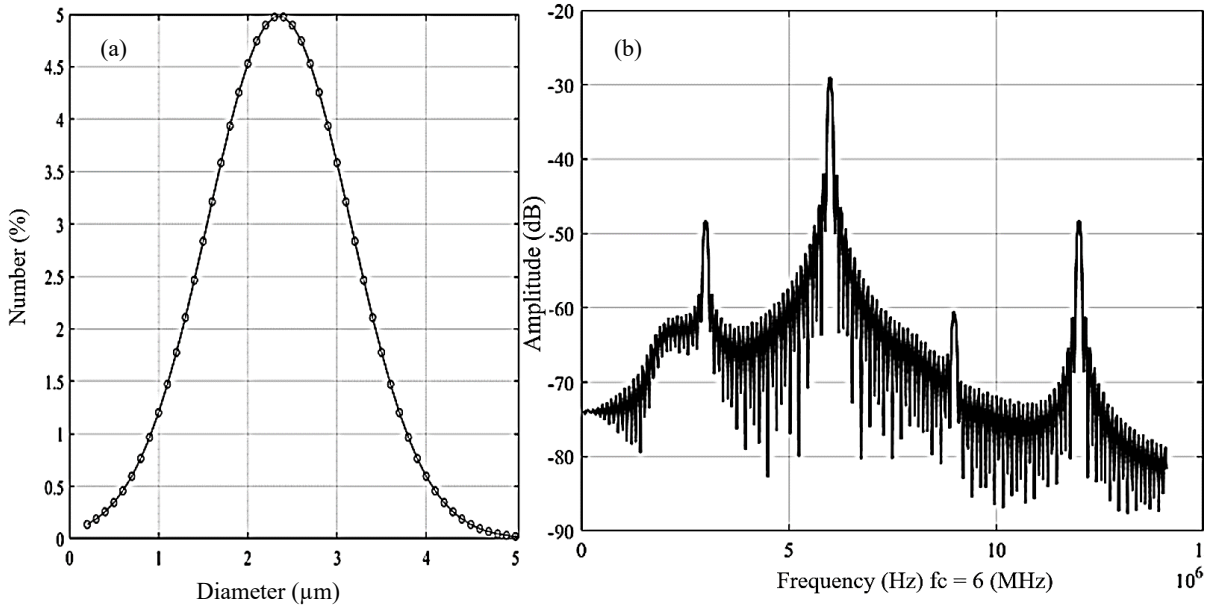

Fig. 6. (a) Gaussian distribution of microbubbles with the mean radius of 1.2 μm and standard deviation of 0.4 μm and (b) Frequency response of microbubbles with this distribution under a driving pressure of 0.28 MPa.

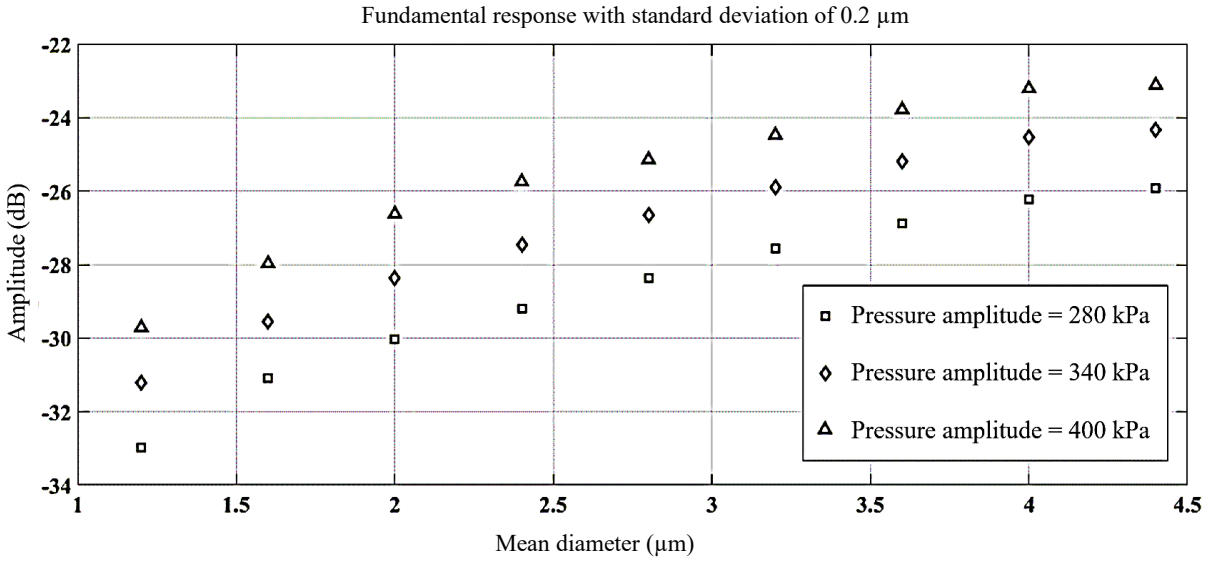

Fig. 7. Fundamental response of the population of SonoVue microbubbles in terms of mean distribution value for different excitation pressure amplitude in 6 MHz excitation frequency.

Figs. 9 and 10 show the effect of excitation frequency on the fundamental and subharmonic responses for the mean radius parameter. It is observed that with decreasing stimulation frequency, the fundamental response increases. Moreover, as the excitation frequency increases, the subharmonic response first decreases. For example, in Fig. 10, the subharmonic response at frequency 6MHz first increases and reaches a peak value within a mean radius of 1 µm and then decreases. At an excitation frequency of 8 MHz, the peak value reaches a mean radius of 0.8 µm. Moreover, at the excitation frequency of 4MHz, peaks occur in a mean radius of 1.6 micrometers (Fig. 11 shows the peak values). Increasing the excitation frequency causes microbubbles with smaller radii to be needed to amplify the subharmonic and vice versa. Therefore, to improve the subharmonic response at different frequencies, it is better to optimize the distribution of the microbubbles.

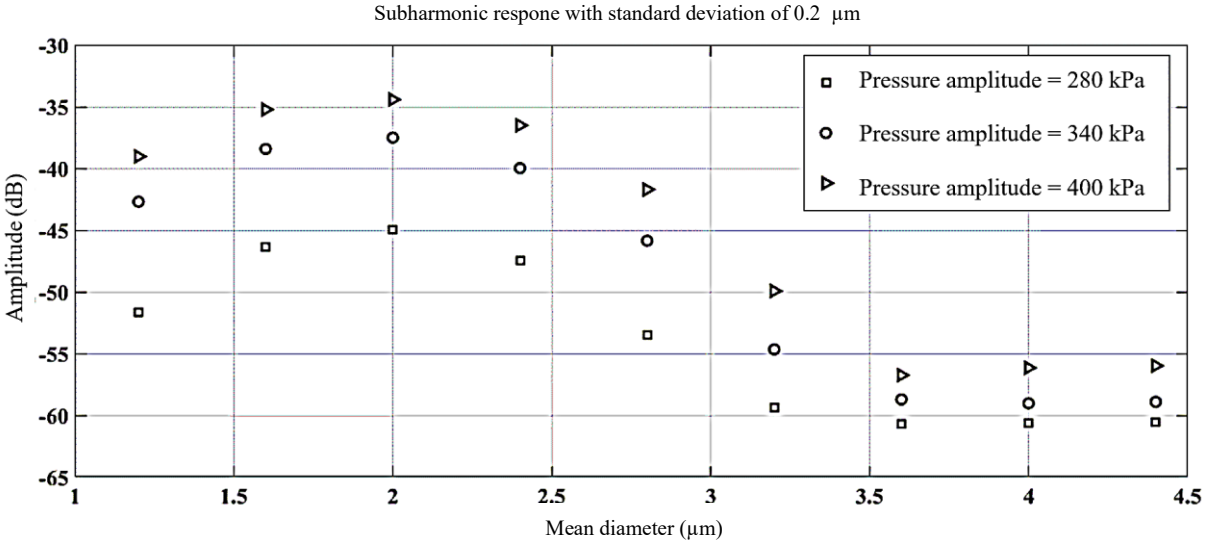

Fig. 8. Subharmonic response of the population of SonoVue microbubbles in terms of mean distribution value for different excitation pressure amplitude in 6 MHz excitation frequency.

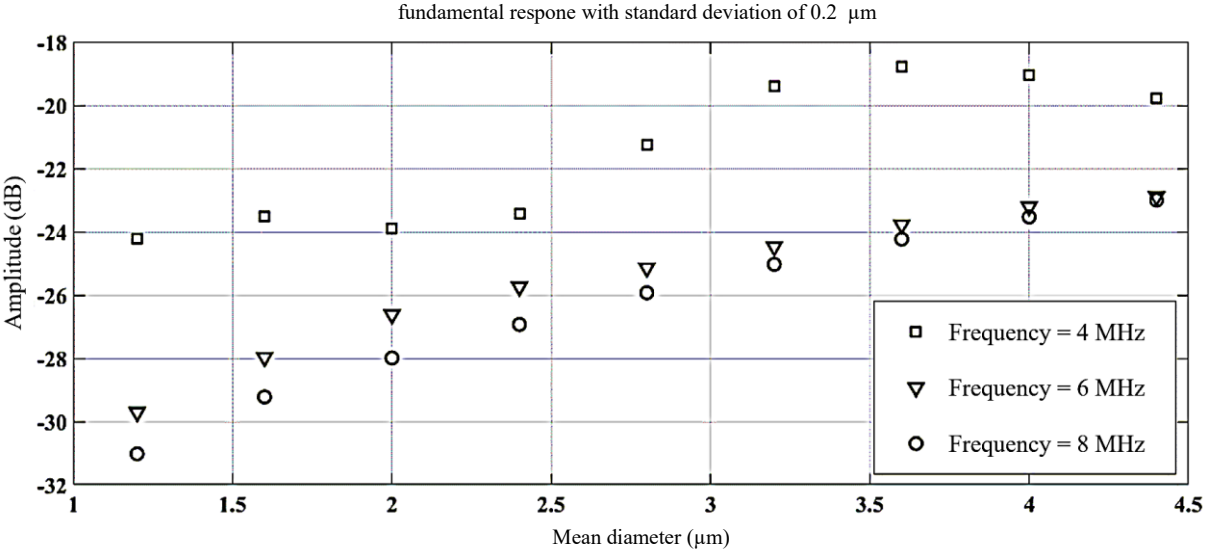

Fig. 9. Fundamental response of the population of SonoVue microbubbles in terms of mean distribution value for different excitation frequencies in 0.4 MPa excitation pressure.

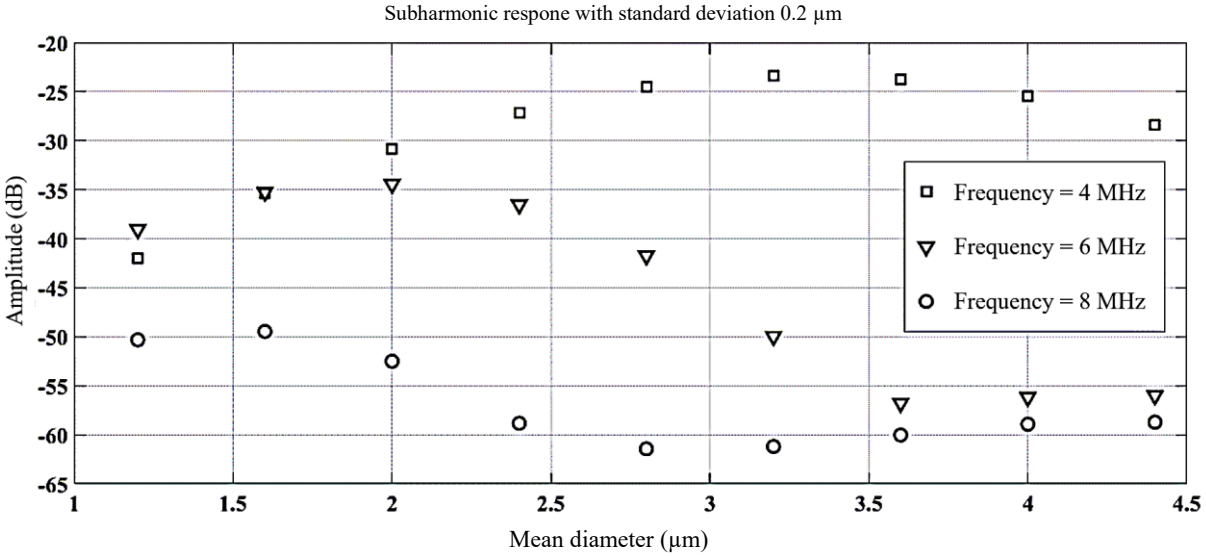

Fig. 10. Subharmonic response of the population of SonoVue microbubbles in terms of mean distribution value for different excitation frequencies in 0.4 MPa excitation pressure.

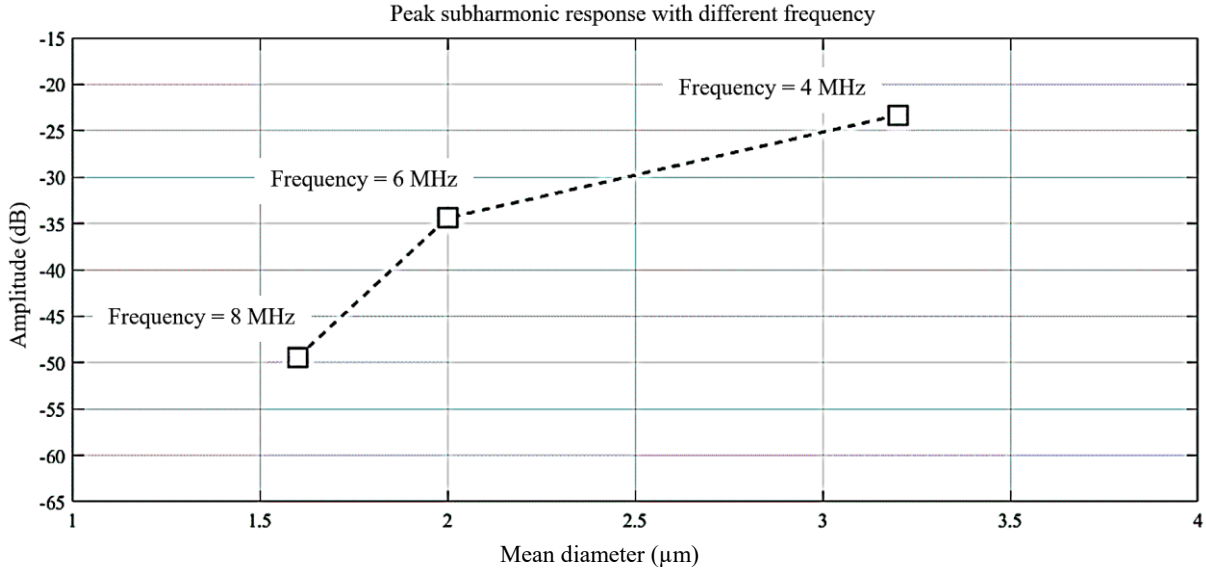

Fig. 11. The peak point of figures of the subharmonic response of microbubbles to different excitation frequencies in excitation pressure amplitude 0.4 MPa and standard deviation 0.2 µm.

By reducing the standard deviation in the radial distribution of microbubbles, we finally reach the limit state without distribution. This condition is called needle distribution. This limit state is shown in Fig. 12. In this figure, reducing the standard deviation puts the radius of the microbubbles around the mean value. For example, with a standard deviation of 0.01 µm, all bubbles are in the radius of 1.59 and 1.61 µm. Fig. 13 shows the frequency response in the distribution cases of Fig. 12. By reducing the standard deviation, the frequency response reaches Fig. 14. Fig. 14 is a non-distributed mode for a radius of 1.6 µm (In the distribution case with a standard deviation of 0.01 µm, Fig. 13 is quite similar to 14).

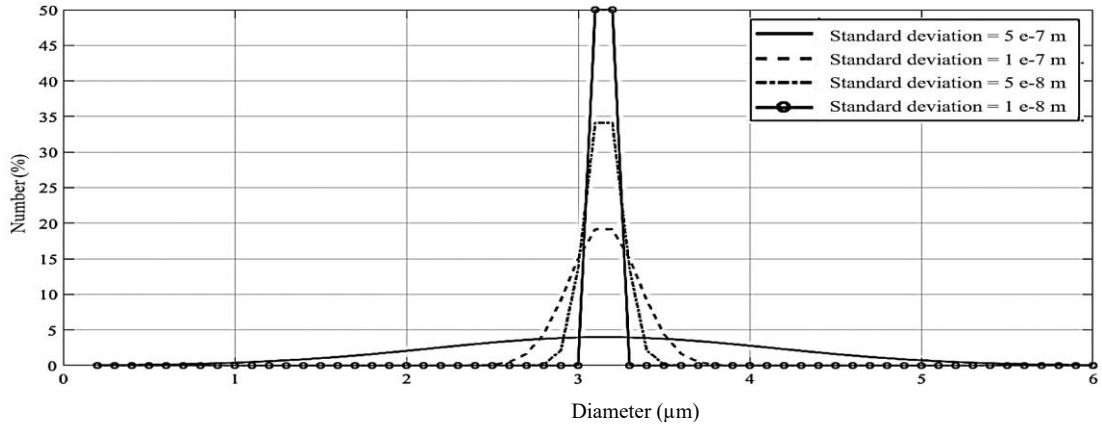

Fig. 12. The size distribution for four different standard deviations, radius range between 0.1 to 3 μm, and mean radius 1.6 μm.

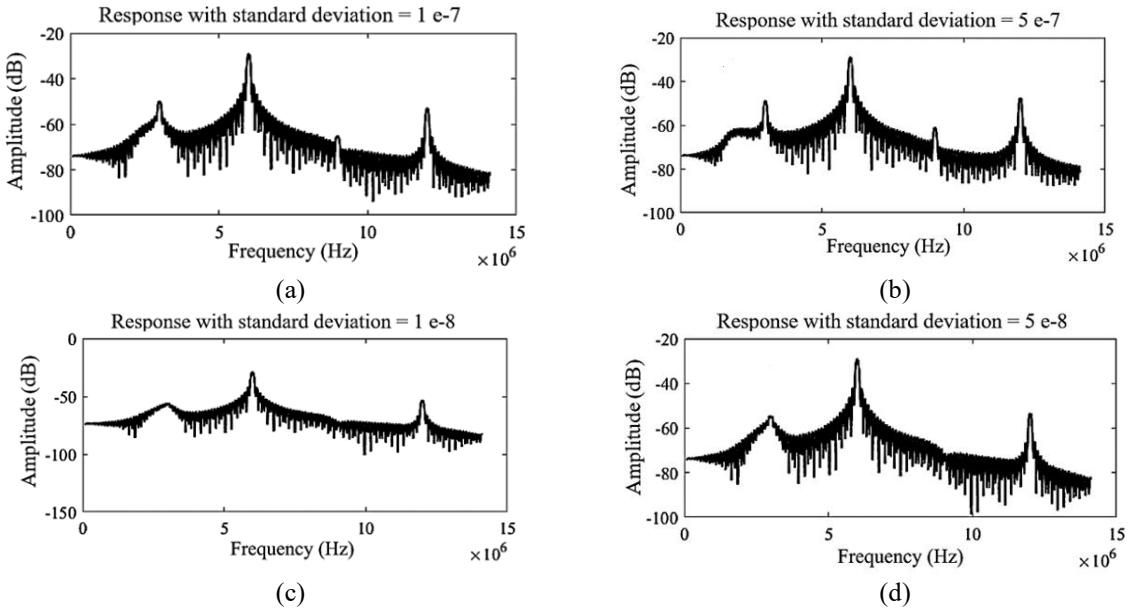

Fig. 13. Frequency responses of SonoVue microbubbles with an incident wave with excitation frequency 6 MHz and pressure amplitude 0.28 MPa and mean radius 1.6 μm. (a) Standard deviation=1e-7m. (b) Standard deviation=5e-7m. (c) Standard deviation=1e-8m. (d) Standard deviation=5e-8m.

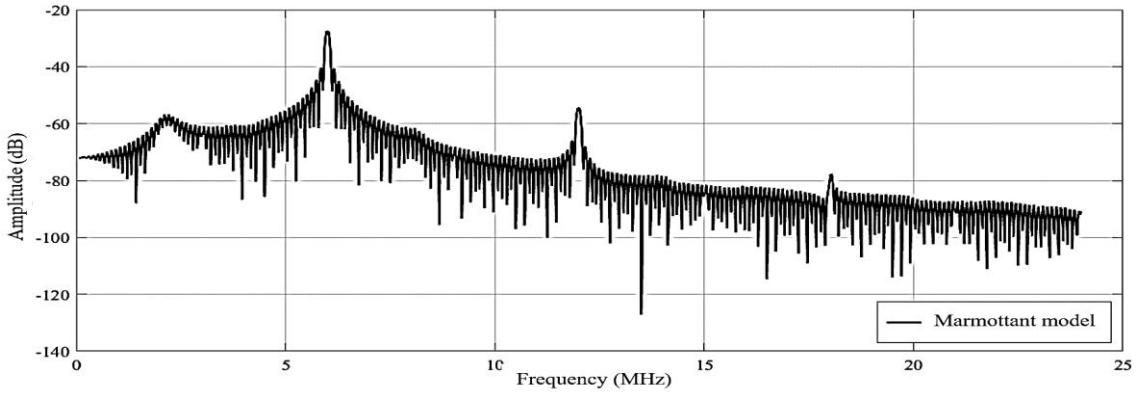

Fig. 14. SonoVue single bubble frequency response in the radius of 1.6 μm and frequency of 6 MHz, and pressure range of 0.28 (MPa).

4. Conclusions

Demographic behaviors of small bubbles exposed to pulsed Ultrasound have not been fully explored. In this study, the effect of the radial distribution of Marmottant shell microbubbles on the frequency response was investigated. It was shown that at each excitation pressure, there is an optimal radial distribution for the subharmonic response. At a constant excitation pressure of 0.4 MPa and a standard deviation of 0.2, the fundamental response increases with increasing mean radius, but the subharmonic response first increases to a peak value and then decreases.

This peak value occurs for 4.6 and 8 MHz frequencies in the mean radii of 0.8.1 and 1.6 μm. It is also observed that the fundamental and subharmonic responses are directly related to the excitation pressure. At a constant excitation frequency, the mean value of the fundamental response increases with increasing radius, and the subharmonic response first increases and reaches its peak value and then decreases. This peak value occurs for radial distributions with a standard deviation of 0.2 μm at frequencies of 4, 6, and 8 MHz and independent of excitation pressure, at a mean radius of 1.6, 1, and 0.8 μm, respectively. The data show that the value of the subharmonic peak occurs less with increasing frequency in the mean radius. In the constant mean radius mode, the subharmonic response is generated and amplified by increasing the standard deviation (increasing the radial range of microbubbles).

In contrast, the fundamental answer is almost constant. It was also shown that the frequency response tends to be a frequency response without distribution by decreasing the standard deviation. According to studies, the radial distribution of microbubbles can be optimized to achieve a more robust subharmonic response. This optimization can be effective in subharmonic imaging. Therefore, controlling the radial distribution of microbubbles can help improve imaging quality.

References

[1] N. De Jong, R. Cornet and C. T. Lancee, “Higher harmonics of vibrating gas-filled microspheres, Part one: simulations”, *Ultrasonics*, Vol. 32, No. 6, pp. 447-453, (1994).

[2] C. C. Church, “The effects of an elastic solid surface layer on the radial pulsations of gas bubbles”, *J. Acoust. Soc. Am*. Vol. 97, No. 3, pp.1510-1521, (1995).

[3] N. De Jong and L. Hoff, “Ultrasound scattering properties of Albunex microspheres”, *Ultrasonics*, Vol. 31, No. 3, pp. 175-181, (1993).

[4] S. M. Van der Meer, B. Dollet, M. M. Voormolen, C. T. Chin, A. Bouakaz, N. De Jong, M. Versluis and D. Lohse, “Microbubble spectroscopy of ultrasound contrast agents”, *J. Acoust. Soc. Am*. Vol. 121, No. 1, pp. 648-656, (2007).

[5] L. Hoff, P. C. Sontum and J. M. Hovem, “Oscillations of polymeric microbubbles: Effect of the encapsulating shell” *J. Acoust. Soc. Am*. Vol. 107, No. 4, pp. 2272-2280, (2000).

[6] D. Chatterjee and K. Sarkar, “A Newtonian rheological model for the interface of microbubble contrast agents”, *Ultrasound in medicine & biology*, Vol. 29, No. 12, pp. 1749-1757, (2003).

[7] P. M. Shankar, P. D. Krishna and V. L. Newhouse, "Subharmonic backscattering from ultrasound contrast agents", *J. Acoust. Soc. Am.*, Vol. 106, No. 4, pp. 2104-2110, (1999).

[8] K. Sarkar, W. T. Shi, D. Chatterjee and F. Forsberg, “Characterization of ultrasound contrast microbubbles using in vitro experiments and viscous and viscoelastic interface models for encapsulation", *J. Acoust. Soc. Am.*, Vol. 118, No. 1, pp. 539-550, (2005).

[9] P. Marmottant, S. Van der Meer, M. Emmer, M. Versluis, N. De Jong, S. Hilgenfeldt and D. Lohse, “A model for large amplitude oscillations of coated bubbles accounting for buckling and rupture”, *J. Acoust. Soc. Am*., Vol. 118, No. 6, pp. 3499-3505, (2005).

[10] F. Forsberg, W. T. Shi and B. B. Goldberg, “Subharmonic imaging of contrast agents”, *Ultrasonics*, Vol. 38, No. 8, pp. 93-98, (2000).

[11] F. Forsberg, J. B. Liu, T. Shi, J. Furuse, M. Shimizu and B. Barry, "In vivo pressure estimation using subharmonic contrast microbubble signals: Proof of concept, IEEE transactions on ultrasonics", *Ferroelectr. Freq. Control*., Vol. 52, No. 4, pp. 581-583, (2005).

[12] P. M. Shankar, P. D. Krishna and V. L. Newhouse, "Advantages of subharmonic over second harmonic backscatter for contrast-to-tissue echo enhancement", *Ultrasound Med. Biol.*, Vol. 24, No. 3, pp. 395-399, (1998).

[13] D. Adam, M. Sapunar and E. Burla, "On the relationship between encapsulated ultrasound contrast agent and pressure", *Ultrasound Med. Biol.*, Vol. 31, No. 5, pp. 673-686, (2005).

[14] K. S. Andersen, J. A. Jørgen, "Impact of acoustic pressure on ambient pressure estimation using ultrasound contrast agent", *Ultrasonics*, Vol. 50, No. 2, pp. 294-299, (2010).

[15] A. Katiyar, K. Sarkar and F. Forsberg, "Modeling subharmonic response from contrast microbubbles as a function of ambient static pressure", *J. Acoust. Soc. Am*., Vol. 129, No. 4, pp. 2325-2335, (2011).

[16] L. M. Leodore, F. Forsberg and W. T. Shi, "P5B-6 In Vitro Pressure Estimation Obtained from Subharmonic Contrast Microbubble Signals", *IEEE Ultrasonics Symposium Proceedings*, pp. 2207-2210, (2007).

[17] M. Overvelde, V. Garbin, J. Sijl, B. Dollet, N. De Jong, D. Lohse and M. Versluis, "Nonlinear shell behavior of phospholipid-coated microbubbles", *Ultrasound Med. Biol.*, Vol. 36, No. 12, pp. 2080-2092, (2010).

[18] T. Sun, N. Jia, D. Zhang and D. Xu, "Ambient pressure dependence of the ultra-harmonic response from contrast microbubbles", *J. Acoust. Soc. Amer.*, Vol. 131, No. 6, pp. 4358-4364, (2012).

[19] R. Basude and M. A. Wheatley, "Generation of ultraharmonics in surfactant based ultrasound contrast agents: use and advantages" *Ultrasonics.*, Vol. 39, No. 6, pp. 437-444, (2001).

[20] P. J. A. Frinking, E. Gaud, J. Brochot and M. Arditi, "Subharmonic scattering of phospholipid-shell microbubbles at low acoustic pressure amplitudes", *IEEE Trans. Ultrason. Ferroelectr. Freq. Control.*, Vol. 57, No. 8, pp. 1762-1771, (2010).

[21] O. Lotsberg, J. M. Hovem and B. Aksum, "Experimental observation of subharmonic oscillations in Infoson bubbles", *J. Acoust. Soc. Am.*, Vol. 99, No. 3, pp. 1366 – 1369, (1996).

[22] H. R. Zheng and R. Shandas, "Gaussian-integration technique to predict backscatter characteristics from ultrasound contrast agents", *IEEE Ultrason. Symp.*, Vol. 3, pp. 1706-1709, (2004).

[23] Yn. Zhang, Zb. Jiang, J. Yuan et al., "Influences of bubble size distribution on propagation of acoustic waves in dilute polydisperse bubbly liquids", *J. Hydrodyn*, Vol. 31, No. 1, pp. 50–57, (2019).

[24] I. G. Newsome, T. M. Kierski and P. A. Dayton "Assessment of the Superharmonic Response of Microbubble Contrast Agents for Acoustic Angiography as a Function of Microbubble Parameters", *Ultrasound Med. Biol.*, Vol. 45, No. 9, pp 2515-2524, (2019).

[25] H. Haghi, A. J. Sojahrood and M. C. Kolios, "Collective nonlinear behavior of interacting polydisperse microbubble clusters", *Ultrason. Sonochem.*, Vol. 58, Article 104708, (2019).

[26] J. E. Streeter, R. Gessner, I. Miles and P. A. Dayton, "Improving Sensitivity in Ultrasound Molecular Imaging by Tailoring Contrast Agent Size Distribution: In Vivo Studies", *Mol. Imag.*, Vol. 9, No. 2, pp. 87-95, (2010).

[27] N. A. Tsochatzidis, P. Guiraud, A. M. Wilhelm and H. Delmas, "Determination of velocity, size and concentration of ultrasonic cavitation bubbles by the phase-Doppler technique", *Chem. Eng.*

Sci., Vol. 56, No. 5, pp. 1831-1840, (2001).
[28] A. Brotchie, F. Grieser and M. Ashokkumar, "Effect of Power and Frequency on Bubble-Size Distributions in Acoustic Cavitation", *Phys. Rev. Lett.*, Vol. 102, No. 8, 084302 (2009).
[29] D. Gubaidullin and Y. Fedorov, "Sound waves in a liquid with polydisperse vapor-gas bubbles", *Acoust. Phys.*, Vol. 62, No. 2, pp. 179-186, (2016).
[30] K. Ando, T. Colonius and C. E. Brennen "Improvement of acoustic theory of ultrasonic waves in dilute bubbly liquids" *J. Acoust. Soc. Am.*, Vol. 126, No. 3, EL69-EL74 (2009).
[31] S. Hilgenfeldt, D. Lohse and M. Zomack, "Response of bubbles to diagnostic ultrasound: a unifying theoretical Approach", *Eur. Phys. J. B*, Vol. 4, No. 2, pp. 247–55, (1998).
[32] M. Versluis, B. Schmitz, A. Von Der Heydt and D. Lohse, "How snapping shrimp snap: through cavitating bubbles", *Sci.*, Vol. 289, No. 5487, 2114–2117, (2000).
[33] C. C. Church, "The effects of an elastic solid-surface layer on the radial pulsations of gas-bubbles", *J. Acoust. Soc. Am.*, Vol. 97, No. 3, pp. 1510–21, (1995).
[34] L. Hoff, P. C. Sontum and J. M. Hovem, "Oscillations of polymeric microbubbles: effect of the encapsulating shell", *J. Acoust. Soc. Am.*, Vol. 107, No. 4, pp. 2272–2280, (2000).
[35] H. Medwin, "Counting bubbles acoustically—review", *Ultrasonics*, Vol. 15, No. 1, pp. 7–13 (1977).
[36] S. H. Bloch, R. E. Short, K. W. Ferrara and E. R. Wisner, "The effect of size on the acoustic response of polymer-shelled contrast agents" *Ultrasound Med. Biol.*, Vol. 31, pp. 439–44, (2005).
[37] K. Soetanto and M. Chan, "Fundamental studies on contrast images from different-sized microbubbles: analytical and experimental studies", *Ultrasound Med. Biol.*, Vol. 26, No. 1, pp. 81–91, (2000).
[38] F. Li, L. Wang, Y. Fan and D. Li, "Simulation of noninvasive blood pressure estimation using ultrasound contrast agent microbubbles", *IEEE Trans. Ultrason. Ferroelectr. Freq. Control.*, Vol. 59, No. 4, pp. 715-726, (2012).
[39] K. Sarkar, W. T. Shi, D. Chatterjee and F. Forsberg, "Characterization of ultrasound contrast microbubbles using in vitro experiments and viscous and viscoelastic interface models for encapsulation", *J. Acoust. Soc. Am.*, Vol. 118, No. 1, pp. 539–550, (2005).

How to cite this paper:

M. Mahdi, M. Shariatnia and M. Rahimi, "Numerical investigation of the effect of size distribution on the frequency response of encapsulated microbubbles,", *J. Comput. Appl. Res. Mech. Eng.,* Vol. 13, No. 1, pp. 89-101, (2023).

DOI: 10.22061/JCARME.2023.8944.2207

URL: https://jcarme.sru.ac.ir/?_action=showPDF&article=1882